Article ID: 1006-8775(2011) 02-0103-10

THE IMPACTS OF ORBITAL PARAMETERS ON SUMMER PRECIPITATION OVER CHINA IN THE HOLOCENE

HUANG Jian-bin (黄建斌)[1], WANG Shao-wu (王绍武)[1], WEN Xin-yu (闻新宇)[1], ZHOU Tian-jun (周天军)[2], ZHU Jin-hong (朱锦红)[3], YANG Bao (杨 保)[4], REN Guo-yu (任国玉)[5]

(1. Department of Atmospheric Sciences, School of Physics, Peking University, Beijing 100871 China; 2. LASG, Institute of Atmospheric Physics, Chinese Academy of Sciences, Beijing 100871 China; 3. Illinois State Water Survey, Department of Natural Resources, University of Illinois at Urbana-Champaign, Champaign, Illinois, USA; 4. Key Laboratory of Desert and Desertification, Chinese Academy of Sciences, Lanzhou 734000; 5. Laboratory for Climate Studies, China Meteorological Administration, Beijing 100081 China)

Abstract: The impact of orbital parameters on the climate of China in the Holocene is simulated from 11kaBP to 0kaBP with an interval of 1ka using National Center for Atmospheric Research (NCAR) Community Atmosphere Model version 2 (CAM2). The geographic distributions of summer precipitation around both 9kaBP and 4kaBP were realistically captured by CAM2, compared to the proxy data collected from 80 stations. Among all orbital parameters, the precession plays a major role in computing solar radiation, which dominates the variations of summer precipitation over China during the Holocene. The summers around 9kaBP were the wettest in China. Later on, the precipitation gradually reduced to the minimum around 0kaBP by about 10%. This tremendous change occurred from the Northeast China and the eastern Inner Mongolia extending southwestwards to the Qinghai-Tibet Plateau, especially over the Qinghai-Tibet Plateau.

Key words: Holocene; climate simulation; orbital parameters; climate humidity

CLC number: P532 **Document code:** A **doi:** 10.3969/j.issn.1006-8775.2011.02.002

1 INTRODUCTION

The Holocene was defined starting from 11.6 cal ka BP (relative to A.D.2000)[1]. So far, we still live in this geological epoch. Studying climate variations and its mechanisms in the Holocene could improve our understanding of present climate change and projection of future climate. Overall, there are three main characteristics in the Holocene: 1) temperature increasing in early and decreasing from the middle to the late Holocene, which appeared especially clear at boreal high latitudes; 2) wet in early, then turning to dry in middle and late Holocene at the middle-low latitudes, especially along the Asia-African monsoon area; 3) rapidly stepping down for nine times into the status of colder and drier than before (abrupt climate changes). China also experienced the similar changes in this period[2].

Shi[3] has studied the temperature variations in the Holocene over China as early as in 1992. After that, Wang[4] reconstructed a temperature time series over China back to 10ka ago based on Shi's data. Compared to temperature, the variations of precipitation over China have not been evenly examined yet, given the lack of data. According to the pollen and other proxy data, Shi[3] pointed out that it was wet during the megathermal maximum. An[5] divided the domain of China into seven subdivisions based on the records of pollen and water level of lakes, and numerical modeling with an interval of 3ka. He studied the variations of climate humidity over China and found that the maximum humidity occurred asynchronously in different regions. Yuan et al.[12] proposed that a stable cycle with a period of 20ka existed in the relation between climate humidity and solar radiation based on stalagmite inferred δO^{18} values in South China. This relationship was also found in the African[13] and Asian monsoon areas[14], where the solar radiation was primarily affected by precession[13, 14]. Due to the sparse proxy data,

Received: 2010-02-12; **Reviced:** 2010-11-27; **Accepted:** 2011-04-15
Foundation item: R&D Special Found for Public Welfare Industry (meteorology) (GYHY200706010); National Science Foundation for Post-doctoral Scientists of China (4131482-051)
Biography: HUANG Jian-bin, Ph.D., primarily undertaking research on climate change and modeling.
Corresponding author: HUANG Jian-bin, e-mail: hjb@pku.edu.cn

detailed temporal and spatial distributions of climate humidity were not available at that moment. And the proxy data even did not cover Xinjiang, Northwest China.

Recently, a number of high resolution and well-dated proxy series were available. In addition, a lot of new regional proxy series have been reconstructed in the past decade, such as in Qinghai-Tibet[8], West China[9], South China[10], Taiwan and South China Sea[11]. This provides us the opportunities to comprehensively examine the past climate changes over China. Based on 23 proxy series, An et al.[6] investigated the climate humidity over Northwest China. Morill et al.[7] also probed the climate humidity changes along the border of Northeast and Northwest China. However, some series are not long enough to cover the whole Holocene.

The goal of this study is to investigate the impacts of orbital parameters on the variations of precipitation in the Holocene over China by comparing the simulations to the up-dated high resolution proxy data. The proxy data represent climate humidity, which involve not only precipitation but also temperature. However, climate models only provide precipitation instead of climate humidity data. Since the annual precipitation is mainly brought by summer monsoon in China, especially over the eastern China, the precipitation in summer plays a key role in climate humidity. Besides, the impact of the uncertainties in simulated temperature might be very complex. Furthermore, to convert precipitation to climate humidity is even more difficult and complicated. Therefore, we will not define a climate humidity index combining the simulated precipitation and temperature here. Instead, the simulated summer precipitation will be analyzed and compared with climate humidity from the proxy data directly to avoid the biases caused by the combination.

This paper is organized as follows. The model and experiments design are described in section 1. Section 2 shows the variations of precipitation by comparing model results with the proxy data. Main conclusions are drawn in section 3.

2 MODEL AND EXPERIMENTS

Since the late 1990s, the climate variations in the Holocene have been examined mostly by global climate models driven by orbital parameters[15, 16] in two ways: equilibrium[15, 16], so-called snapshot or slice, and transient climate simulation[17, 18]. Medium complex climate models were usually used to simulate transient climate due to limited requirement of computational resources[19]. At the beginning of the Holocene, the summer insolation at 65° N achieved its maximum around 10kaBP. After half of the cycle of precession, it almost reached its minimum at present. Comparing to the other two orbital parameters, which are eccentricity and obliquity with the periods of 100ka and 40ka, respectively, the precession dominated the variation of insolation in the Holocene. In view of the major role the precession played, the equilibrium simulations conducted in 12 slices during the Holocene here are named as sensitivity studies of "the impact of precession on Holocene climate" although they were driven by all three orbital parameters.

In this study, the impacts of precession on the climate of the Holocene were simulated from 11kaBP to 0kaBP with an interval of 1ka by NCAR CAM2. NCAR CAM2[20] is a global primitive equation spectral model with T42 triangular truncation in the horizontal (2.8° ×2.8° , which is about 300 km) T42 grid and 26 vertical levels. (Details of the model are described online at the NCAR Website: http://www.ccsm.ucar.edu/models/ccsm2.0.1/cam/camUsersGuide/.) Compared to its earlier version CCM3, CAM2 incorporates significant improvements to its physical parameterizations[21, 22]. It has already been widely used in studies of climate by numerical modeling and sensitivity experiments. Here, the model is driven only by orbital parameters, namely eccentricity, obliquity, and precession, which are derived from Berger's results[23, 24]. In addition, the CO_2 concentration is kept constant in all experiments, which was adopted as the mean of the Holocene (corresponds to the value of CO_2 concentration in mid-Holocene). Each of the 12 slices has been integrated for 15 years, the first five years were cut off as spin-up and the average of the remaining 10 years was analyzed.

3 SUMMER PRECIPITATION IN THE HOLOCENE

In this section, the variations of summer precipitation in the Holocene will be examined by comparing the simulations with a variety of proxy data over the entire China. Due to the differences between the eastern and western China, the summer precipitation will also be investigated individually in these two regions. Its spatial distributions at 9kaBP and 4kaBP are presented at the end of this section.

3.1 *Summer precipitation over China*

Figure 1 presents the simulated anomalies of summer precipitation relative to the average of the precipitation in the 12 slices. The northeast-southwest band with the positive anomaly gradually shifted southward from North China to South China. For further examination of the spatial and temporal variations, EOF (Empirical Orthogonal Function) analysis was performed to the summer precipitation

(Fig. 2). The leading EOF mode explained 75.8% of the total variance[2]. In this mode, the positive anomaly belt, extending from the Northeast China and the eastern Inner Mongolia through North China and Hetao region to the Qinghai-Tibet Plateau (dashed line in Fig. 2), matched the band in Fig. 1 well. In particular, the descent of the corresponding time series was consistent to the variations of summer insolation at 65° N, peaked at 11–10kaBP and reached the lowest at 1–0kaBP (Fig. 3). This consistency implied that the distribution of summer rainfall was very sensitive to the orbital parameters. This leading mode, which explained more than 3-quarter variance (75.8%), indicated the major features of summer rainfall in the Holocene caused by the changing precession[2]. It also illustrated that the Tibetan Plateau was the most sensitive region to the precession.

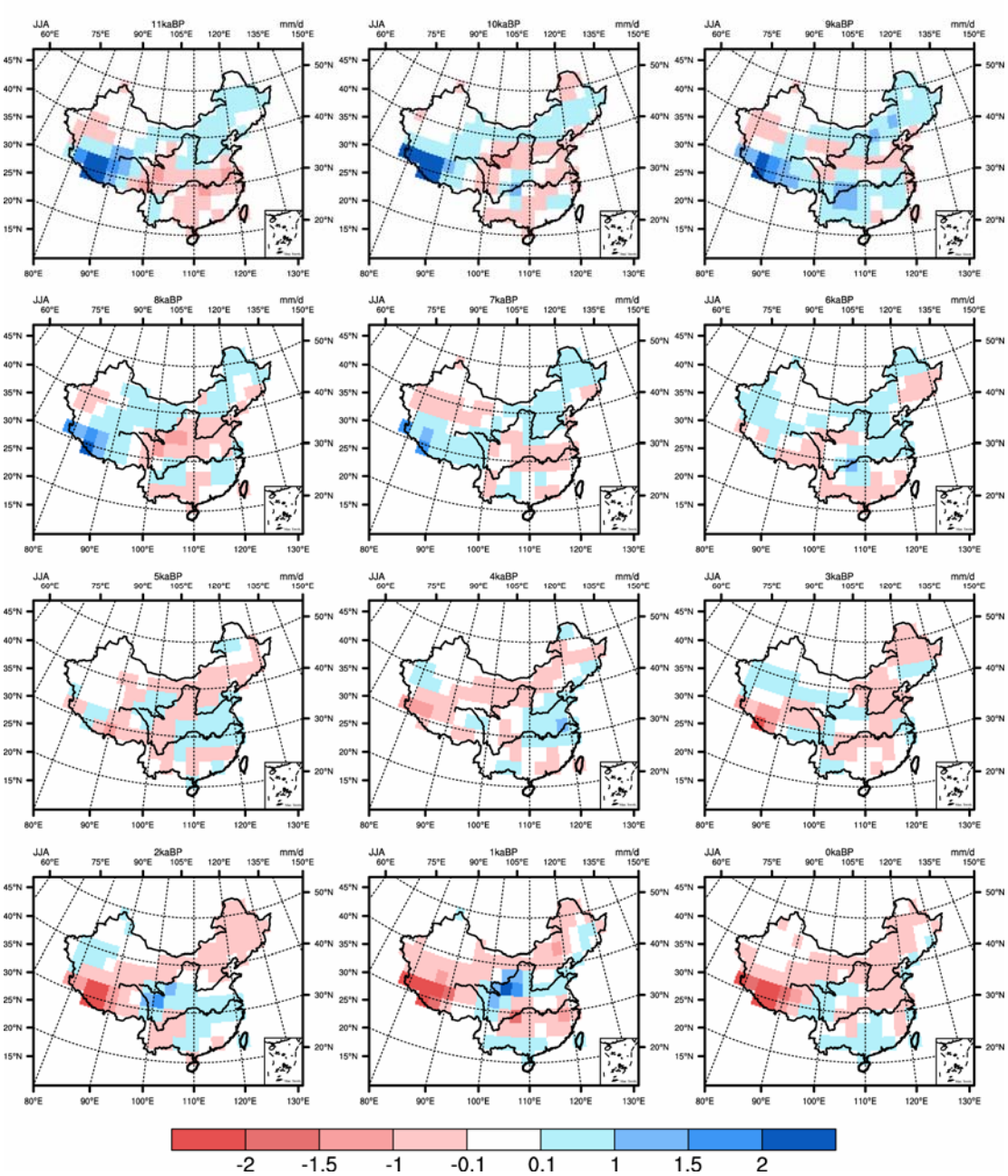

Fig. 1. The simulated summer rainfall anomalies in each of the 12 slices in the Holocene relative to their average. Unit: mm day^{-1}

The maximum (514 mm) of the simulated summer rainfall over the entire China occurred at 9kaBP, and then gradually reduced to its minimum (464 mm) at 0kaBP (Fig. 3) by about 50 mm (10%). Some studies[3, 5] proved that the summer rainfall decreased by 20%–30% in some typical areas in the Holocene. Regarding the differences of the areas where the studies was conducted above, the simulated reduction of summer rainfall is considered consistent to the previous studies[3, 5]. In addition, it is very impressive that the trend of insolation changes at 65° N was identical to that of summer rainfall of China. It

suggested that the variation of the summer rainfall of China in the Holocene was primarily induced by the precession changes. The similar trend in PC1 implied that the variations of summer rainfall caused by the changed precession were mainly represented by the shift of the Northeast-Southwest band.

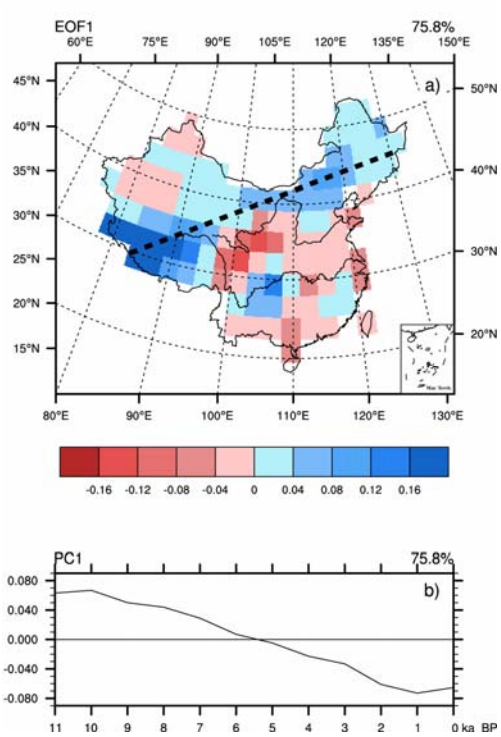

Fig. 2. The leading mode (EOF1) of the simulated summer precipitation over China in the Holocene (a); the corresponding time series PC1 (b). The dashed line represents the Northeast-Southwest band covering Northeast China, the east of Inner Mongolia, North China, Hetao region and the Qinghai-Tibet Plateau. (After Wang et al.[2])

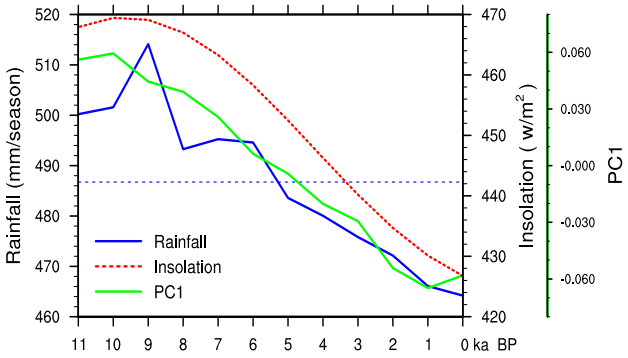

Fig. 3. The average of the simulated summer rainfall over China in the Holocene (blue solid line), Units: mm season^{-1}; the summer insolation variations at 65° N (red dot line). Units: w m^{-2}; the green line is the PC1 in Fig. 2.

3.2 *Summer precipitation over the eastern China*

According to the proxy data based on the pollen and lake levels and simulations, An[5] divided the domain of China into seven sections. His research showed that the variations of the humidity in different regions of China were not simultaneous. In this paper, the domain of China was divided into six subdomains (Fig. 4) in terms of the climate features of China and the simulations (Fig. 1). Each of these six subdomains covers the similar area as An's corresponding one[5], but not identical.

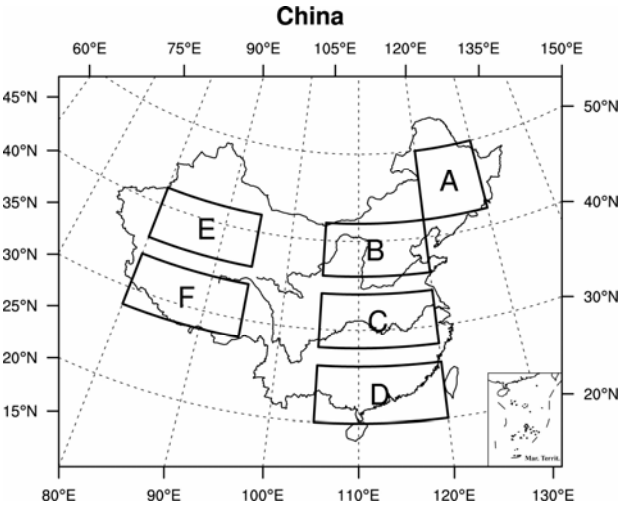

Fig. 4. Six subdomains of China in this paper. A (120–130° E, 42–50° N), B (105–120° E, 36–42° N), C (105–120° E, 28–34° N), D (105–120° E, 20–26° N), E (80–95° E, 36–42° N), F (80–95° E, 28–34° N)

Domain A, Northeast China, covers three provinces of Heilongjiang, Jilin and Liaoning, and the eastern part of Inner Mongolia Autonomous Region. An[5] pointed out that it was wet there around 14–11kaBP and 13–8kaBP (cal yr) according to the proxy data derived from the archives of pollen and lake level status. We examined the simulation covering the period only from 11kaBP to 0kaBP in our study. In Fig. 5a-A, the simulated wet condition during 11–9kaBP in subdomain A was very similar to An's findings[5], although the major wet period in An's was just beyond our simulations. Domain B was named as the northern-eastern part of East China division by An[5], which covered from the northern part of Huaihe River to the southern part of Northeast China surrounding the Bohai Sea. The simulations presented that it was wet around 10–9kaBP and 9kaBP, proved by the proxy data[5] (Fig. 5a-B). An's simulations[5] also showed the consistency in this wet time. In addition, the simulations also implied the wet climate during 7–6kaBP, also found in the proxy data[5]. For domain C, the proxy data[5] indicated that it was humid in 9–8kaBP and 7kaBP. This was realistically captured by our simulations which showed that during 9kaBP and 6–4kaBP, the Yangtze R. valley experienced excessive precipitation (Fig. 5a-C). Meanwhile, An's work[5] also implied that it was wet in 6kaBP in this region in his experiments. In addition, the data based on pollen[5] observed that the wettest condition in subdomain D occurred at 3kaBP. The simulated summer rainfall increased since 3kaBP

and reached its maximum during 2–0kaBP (Fig. 5a-D), which was somewhat consistent with the proxy data.

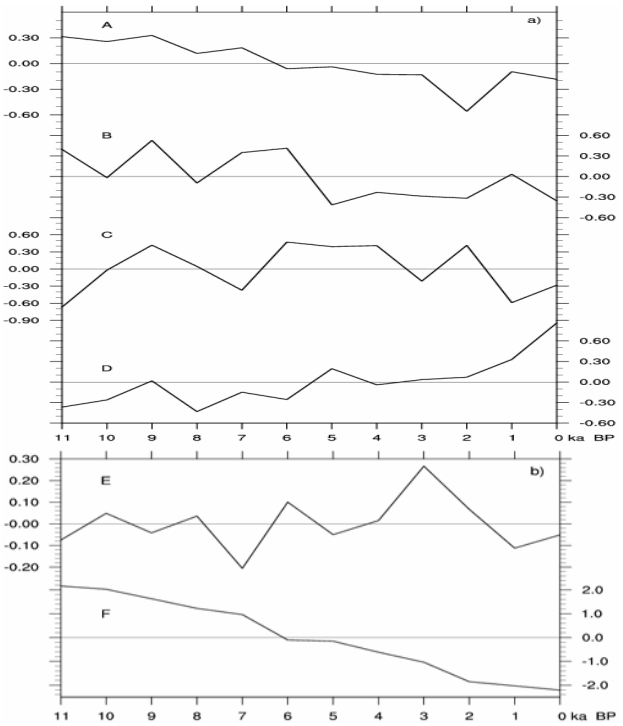

Fig. 5. The simulated variations of summer precipitation anomalies in six subdomains (among them, 4 in the eastern China shown in Fig. 5a and 2 in the western China shown in Fig.5b) described in Fig. 4 for the 12 slices in the Holocene relative to its average, denoted by the horizontal line

3.3 *Summer precipitation over the western China*

Chen[25] indicated that the variations of climate humidity was very different in the westerly wind area of Asian inland and monsoon area of East China. Recently, Chen[26] found that droughts occurred during 11–8kaBP and the maximum humidity existed during 8–5kaBP through proxy data in the central Asia, Xinjiang of China and Mongolia. On the contrary, the eastern China suffered excessive rainfall during 11–8kaBP and drought during 5–2kaBP.

As shown in Fig. 5b-E, the dry condition in 11–7kaBP and wet condition in 6–3kaBP were simulated clearly, which indicated an obviously wet trend in the Holocene suggested by Chen[26]. In addition, the variation of summer rainfall over the Tibetan Plateau (Fig. 5b-F) followed PC1 very well (Fig. 2), implying the significant impact of precession on domain F.

3.4 *Wet/dry distribution at 9kaBP and 4kaBP*

Although the comprehensive studies on climate humidity in the Holocene have been conducted and a number of climate humidity series were published in recent years, it is still difficult to map the geographic distribution of climate humidity over the entire China. In order to improve our understanding of the variations of climate humidity in the Holocene, two slices, which are 9kaBP and 6kaBP, were usually further investigated as the early and middle Holocene in paleoclimate research, respectively[27, 28]. However, in this paper, 9kaBP and 4kaBP were examined as the early and late Holocene, which are generally considered as a typical wet and dry periods, respectively.

During the past several years, much great progress has been made in reconstructing the Holocene climate humidity over China. An[6] mapped dry/wet distribution over Northwest China based on 23 paleoclimate proxy series, but not including the rest of China due to the lack of data. Huang[29] examined plenty of pollen proxy series, most of which were in literature and recorded with $\delta^{14}C$ chronology. However, this is far too enough for describing the distribution of climate humidity in the Holocene over China. Based on as much proxy data as possibly collected, here we qualitatively mapped the dry/wet distribution over the whole China. These proxy data included about 80 series, consisting of pollen, TOC, $\delta^{13}C$ etc. (details shown in Table 1), calibrated by tree ring. 54 out of these 80 proxy series were from pollen. All data were categorized into three groups, wet, normal and dry. Each of them included 1/3 of all events, which were completely covered by these three categories. Following this definition, the wet/dry distribution was mapped in 9kaBP and 4kaBP.

The summer precipitation in the Holocene was also investigated by comparing the simulations to the proxy data. The proxy data indicated that it was wet at 9kaBP and then became dry at 4kaBP in China except the middle and lower reaches of the Yangtze River Valley (Figs. 6a & 6b)[2], which was also exhibited in the simulations (Figs. 6c & 6d). It was noticeable that the wet band from the northeast China and the east of Inner Mongolia Autonomous Region to the Qinghai-Tibet Plateau existed in the proxy data at 9kaBP. Later on, this area experienced a drought period at 4kaBP. In addition, the proxy data also showed the wet condition at 9kaBP in the northern part and dry condition in the southern part of East China. This pattern reversed at 4kaBP. The proxy data demonstrated that the West China experienced drought over the northern part and wet over the southern part at 9kaBP, and the southern part became dry at 4kaBP. The pattern in which the precipitation in northern part was out of phase with that in southern part and its reverse were also reasonably reproduced by CAM2 (Figs. 6c & 6d).

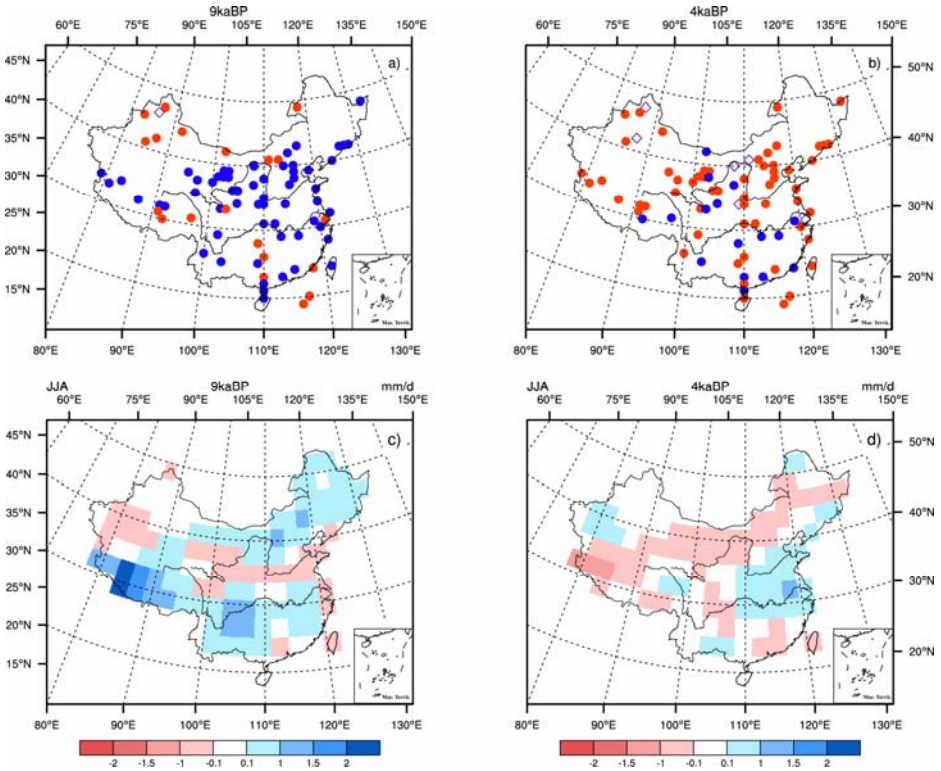

Fig. 6. Geographic distribution of dry/wet at 9kaBP (a) and 4kaBP(b) based on proxy data (blue dot: wet; red dot: dry and diamond: normal). The simulated precipitation anomaly distribution at 9kaBP (c), 4kaBP (d). Units: mm day^{-1} (After Wang et al.[2])

In summary, the summer rainfall increased over the northern part and decreased over the southern part of East China in the Holocene. Meanwhile, the changes were opposite over West China excluding the northern Xinjiang region of China (Fig. 5). In this paper, the early and late Holocene was represented by two time slices of 9kaBP and 4kaBP, respectively. The atmospheric circulations in these two slices were also examined to see if they responded to precession over China in the Holocene. The simulations showed that the East Asian summer monsoon (EASM) was strong in the early Holocene, caused by the intense contrast of sea level pressure (SLP) between the Asian continent dominated by the negative anomaly of SLP and the western Pacific Ocean prevalent with the positive one (Fig. 7a). The opposite pattern suppressed the intensity of the EASM in the late Holocene (Fig. 7b).

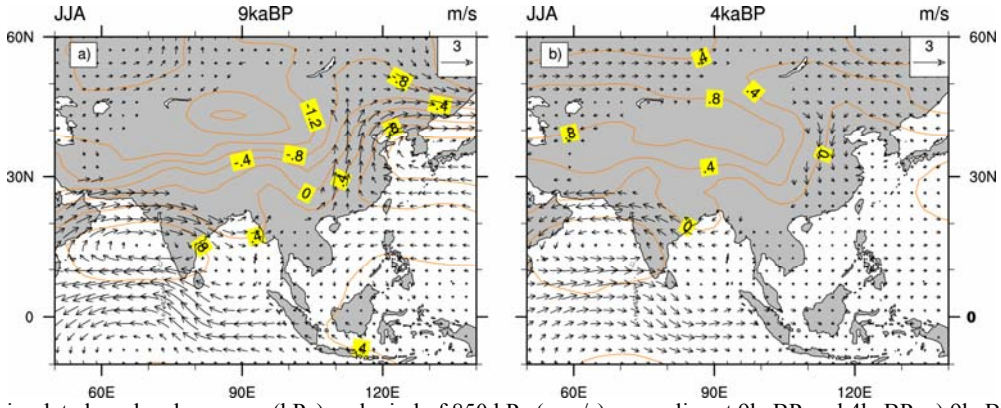

Fig. 7. The simulated sea level pressure (hPa) and wind of 850 hPa (mm/s) anomalies at 9kaBP and 4kaBP. a) 9kaBP; b) 4kaBP

In the early Holocene, the strong EASM brought excessive precipitation to the northern part and reduced convergence of water vapor in the southern part of East China. In the late Holocene, the EASM was getting weak and kept the southern part wet and left the northern part dry. Due to the insolation changes in boreal hemisphere, the geopotential height at 500 hPa was higher in the early Holocene and lower in the late Holocene. During the early Holocene, the cyclonic anomaly dominated the Plateau (Fig. 7c), while the southwest wind enhanced and transported water vapor farther into the southern part of the

plateau. Less water vapor was transported to the northern part of the plateau because of the westerlies weakened by the east wind anomaly. The distribution of circulations and precipitation in the late Holocene was opposite to the early one, which might be attributable to the solar radiation induced by the change of precession.

4 CONCLUSIONS

(1) In the Holocene, the Northeast-Southwest band of summer precipitation, extending from Northeast China, the eastern Inner Mongolia Autonomous Region, North China and Hetao region to the Tibetan Plateau, existed in the proxy data and was reasonably simulated by CAM2. Its noticeable shifts, resulting from the impact of precession, were also revealed in both the proxy data and the simulations.

(2) During the Holocene, it was wet in its early period and dry in the later time. The precipitation dropped by 10%. The simulations demonstrated that this change was caused mainly by the orbital parameters.

(3) The variation of the summer precipitation over North and Northeast China, which was out of phase with that over South and Southwest China in the Holocene, was realistically captured by CAM2. Typically, Tibetan Plateau was the area where the summer precipitation was the most sensitive to the precession.

(4) Among all orbital parameters, the precession was the dominant factor controlling the incoming solar radiation in the Holocene. As a result, the variations of summer rainfall may be induced mainly by precession.

(5) More numerical studies are strongly encouraged for better understanding the climate changes in the Holocene. The improvements in the models for paleoclimate researches, such as considering ocean-land-air interactions and employing high-resolution, are crucial to reproducing the paleoclimate and revealing its mechanisms in the Holocene.

REFERENCES:

[1] JANSEN E E, OVERPECK J, BRIFFA K R, et al. Palaeoclimate [C]// Climate Change 2007: The Physical Science Basis. Contribution of Working Group I to the Fourth Assessment Report of the Intergovernmental Panel on Climate Change, SOLOMON S, QIN D, MANNING M, et al.(eds.) Cambridge and New York: Cambridge University Press, 2007.

[2] WANG Shao-wu, HUANG Jian-bin, WEN Xin-yu, et al. Two modes of summer precipitation variation of Holocene in China [J]. Quatern. Sci., 2009, 29(6): 1 086-1 094 (in Chinese).

[3] SHI Ya-feng, KONG Zhao-chen (eds). The Climates and Environments of Holocene Megathermal in China [M]. Beijing: China Ocean Press, 1992, 1-211 (in Chinese).

[4] WANG Shao-wu, GONG Dao-yi, ZHU Jin-hong. Twentieth-century climatic warming in China in the context of the Holocene [J]. The Holocene, 2001, 11(3): 313-321.

[5] AN Z, PORTER S C, KUTZBACH J E, et al. Asynchronous Holocene optimum of the east Asia monsoon [J]. Quatern. Sci. Rev., 2000, 19(8): 743-762.

[6] AN C B, FENG Z D, BARTON L. Dry or humid? Mid-Holocene humidity changes in arid and semi-arid China [J]. Quatern. Sci. Rev., 2006, 25: 351-361.

[7] MORRILL C, OVERPECK J T, COLE J E. A synthesis of abrupt changes in the Asian summer monsoon since the last deglaciation [J]. The Holocene, 2003, 13: 465-476.

[8] SHEN Cai-ming, LIU Kam-biu, TANG Ling-yu, et al. Quantitative relationships between modern pollen rain and climate in the Tibetan Plateau [J]. Rev. Paleobot. Palynol., 2006, 140: 67-77.

[9] AN C B, TANG L, BARTON L, et al. Climate change and cultural response around 4000 cal yr B. P. in the western part of Chinese Loess Plateau [J]. Quatern. Res., 2005, 63(3): 347-352.

[10] ZHOU Wei-jian, YU Xue-feng, JULL A J T, et al. High-resolution evidence from southern China of an early Holocene optimum and a mid-Holocene dry event during the past 18,000 years [J]. Quatern. Res., 2004, 62: 39-48.

[11] HUANG Chi-Yue, LIEW Ping-mei, ZHAO Mei-xun, et al. Deep sea and lake records of the Southeast Asian paleomonsoons for the last 25 thousand years [J]. Earth Planet. Sci. Lett., 1997, 146: 59-72.

[12] YUAN Dao-xian, CHENG Hai, EDWARDS R L, et al. Timing, duration and transitions of the last interglacial Asian monsoon [J]. Science, 2004, 304: 575-578.

[13] HOELZMANN P, GASSE F, DUPONT L, et al. Palaeoenvironmental Changes in the arid and subarid belt (Sahara-Sahel-Arabian Peninsula) from 150 kyr to present [M]// Battarbee R W, Gasse F, Stickley C E (eds). Past Climate Variability through Europe and Africa. Dordrecht: Springer, 2004, 219-256.

[14] STAUBWASSER M. An overview of Holocene South Asian monsoon records-monsoon domains and regional contrasts [J]. J. Geol. Soc. India, 2006, 68: 433-446.

[15] HEWITT C D, MITCHELL J F B. A fully coupled GCM simulation of the climate of the mid-Holocene [J]. Geophys. Res. Lett., 1998,25: 361-364.

[16] LIU Z, BRADY E, JYNCH-STIEGLITZ J. Global ocean response to orbital forcing in the Holocene [J]. Paleoceanogr., 2003, 18(2), 1041, 20pp.

[17] WEBER S L, CROWLEY T, VAN DER SCHRIER G. Solar irradiance forcing of centennial climate variability during the Holocene [J]. Clim. Dyn., 2004, 22: 539-553.

[18] RENSEN H, GOOSSE H, FICHEFET T, et al. Simulating the Holocene climate evolution at northern high latitudes using a coupled atmosphere-sea ice-ocean-vegetation model [J]. Clim. Dyn., 2005, 24: 23-43.

[19] CLAUSSEN M, MYSAK L A, WEAVER A J, et al. Earth system models of intermediate complexity: closing the gap in the spectrum of climate system models [J]. Clim. Dyn., 2002, 18: 579-586.

[20] KIEHL J T, HACK J J, BONAN G B, et al. The National Center for Atmospheric Research Community Climate Model: CCM3 [J]. J. Climate., 1998, 11: 1 131-1 150.

[21] BLACKMON M B, BOVILLE B, BRYAN F, et al. The Community Climate System Model [J]. Bull. Amer. Meteor. Soc., 2001, 82: 2 357-2 376.

[22] COLLINS W D, RASCH P J, BOVILLE B A, et al. The formulation and atmospheric simulation of the Community

Atmosphere Model: CAM3 [J]. J. Climate, 2006, 19: 2 144-2 161.
[23] BERGER A L. Long-term variations of daily insolation and Quaternary climatic changes [J]. J. Atmos. Sci., 1978, 35: 2 362-2 367.
[24] BERGER A L, LOUTRE M F, LASKAR J. Stability of the astronomical frequencies over the Earth's history for paleoclimate studies [J]. Science, 1992, 255: 560-566.
[25] CHEN Fa-hu, HUANG Xiao-zhong, YANG Mei-lin, et al. Westerly dominated Holocene climate model in arid central Asia-Case study on Bosten Lake, Xinjiang, China [J]. Quatern. Sci., 2006, 26: 881-887 (in Chinese).
[26] CHEN Fa-hu, YU Zi-cheng, YANG Mei-lin, et al. Holocene moisture evolution in arid central Asia and its out-of-phase relationship with Asian monsoon history [J]. Quatern. Sci. Rev., 2008, 27(3-4): 351-364.
[27] CLSAUSSEN M. Simulation of Holocene climate change using climate-system models [M]// MACKAY A, BATTARBEE R, BIRKS J, et al.(eds) Global Change in the Holocene. New York: Orford University Press, 2003, 422-434.
[28] BRACONNOT P, HARRISON S, JOUSSAUME S, et al. Evaluation of PMIP coupled ocean-atmosphere simulations of the mid-Holocene [M]// BATTARBEE R W, GASSE F, STICKLEY C E (eds). Past Climate Variabikity through Europe and Africa. Doraecht: Springer, 2004, 515-533
[29] HUANG Zhen-guo, ZHANG Wei-qiang, et al. Comparative Study of Environmental Evolution during the Holocene in China and Japan [M]. Guangzhou: Guangdong Science and Technology Press, 2002, 1-806 pp.

Citation: HUANG Jian-bin, WANG Shao-wu, WEN Xin-yu et al. The impacts of orbital parameters on summer precipitation over China in the Holocene. *J. Trop. Meteor.*, 2011, 17(2): 103-112.

Appendix 1[2]

Table 1 Data sources selected

	Site	Proxy	Reference	N°	E°	9ka	4ka
1	Hulun Lake	pollen	Chen, et al.[1]	49	118	-	-
2	Qingdeli	pollen	An, et al.[2]	48	133	+	-
3	Wulungu Lake	pollen	Chen, et al.[1]	47	87	-	0
4	Manas Lake	pollen	An C-B, et al. [3]	46	86	0	-
5	Aibi Lake	pollen	An C-B, et al. [3]	45	83	-	-
6	Balikun Lake	pollen	Han and Qu [4]	44	92	-	-
7	Haoluku	LOI	Liu,et al. [5]	43	117	+	-
8	Bosten Lake	pollen	Chen, et al.[1]	42	87	-	0
9	Juyan Lake	pollen	Chen, et al. [1]	42	102	-	+
10	Lake Bayanchagan	pollen	Jiang, et al. [6]	42	115	+	-
11	Jingchuan	pollen	An, et al.[2]	42	126	+	-
12	Hani peat	δ13C	Hong, et al. [7]	42	127	+	-
13	Changbai Mts.	pollen	Huang, et al. [8]	42	128	+	-
14	Tarim	grain size	Feng, et al. [9]	41	85	-	-
15	Chasuqi	pollen	Wang and Sun [10]	41	111	-	0
16	Daihai Lake	TOC	Xiao, et al. [11]	41	113	-	-
17	Yanhaizi Lake	TOC	Chen C-T A, et al. [12]	40	108	+	0
18	Yanggao	pollen	Huang, et al. [8]	40	114	+	-
19	Beijing	pollen	Huang, et al. [8]	40	116	+	-
20	Dagu Mt.	pollen	Huang, et al. [8]	40	124	+	-
21	Alashan Plateau	pollen	Chen, et al. [13]	39	102	+	-
22	Lake Yiema	MS	Chen, et al. [14]	39	103	+	-
23	Baiyangdian	pollen	An, et al. [2]	39	116	+	-
24	Maohebei	pollen	An, et al. [2]	39	119	+	-
25	Dunde	ice core	Liu et al. [15]	38	95	+	-
26	Lake Luanhaizi	pollen	Herzschuh, et al. [16]	38	101	+	-
27	Hongshui River	pollen	Ma, al. [17]	38	102	+	-
28	Zhuyeze Lake	pollen	Chen, et al. [18]	38	103	+	+
29	Yulin	pollen	An, et al. [2]	38	110	+	-
30	Suning	grain size	Yin, et al. [19]	38	116	+	-
31	Hurleg Lake	pollen	Zhao, et al. [20]	37	97	+	-
32	Qinghai Lake	pollen	Liu, et al. [21]	37	100	+	-
33	Liushuwan	pollen	Li, et al. [22]	37	108	+	+
34	Neiqiu	grain size	Yin, et al. [19]	37	115	+	-
35	Baxie	MS	An, et al. [2]	36	104	+	-
36	Sujiawan	TOC	An C-B, et al. [23]	36	105	+	-
37	Qingdao	pollen	Wang, et al. [24]	36	120	+	-
38	Tibetan Plateau	pollen	Shen, et al. [25]	35	97	+	-
39	Fuping	pollen	An, et al. [2]	35	110	+	-
40	Lake Bangong	δ13C	Fontes, et al. [26]	34	79	+	-
41	Guliya	accumulation	Thompson, et al. [27]	34	83	+	-
42	Dadiwan	TOC	An C-B, et al. [23]	34	105	+	+

43	Liwan	MS	Pang, et al. [28]	34	109	+	0
44	Beizhuangcun	pollen	An, et al. [2]	34	110	+	-
45	Wuyang	pollen	Huang, et al. [8]	34	114	+	-
46	Jianhu	pollen	An, et al. [2]	34	120	+	-
47	Sumxi Co Lake	pollen	Gasse, et al. [29]	33	81	+	-
48	Zoige	TOC	Zhou, et al. [30]	33	102	+	-
49	Hongyuan peat	δ13C	Hong, et al. [7]	33	103	-	+
50	Selin Co Lake	δ13C	Gu, et al. [31]	32	87	+	-
51	Lake Zigetang	pollen	Herzschuh, et al. [32]	32	91	+	-
52	Ahung Lake	δ13C	Morrill, et al. [33]	32	92	+	-
53	Qidong	pollen	An, et al. [2]	32	122	+	-
54	Luoe Lake	TOC	Wu, et al. [34]	31	91	-	-
55	Ren Co Lake	pollen	Tang, et al. [35]	31	97	-	+
56	Shanbao Cave	δ18O	Shao, et al. [36]	31	110	+	-
57	Jingmen	pollen	Huang, et al. [8]	31	112	+	-
58	Wuhu	pollen	Huang, et al. [8]	31	119	+	+
59	Shanghai	pollen	Cai, et al. [37]	31	121	-	0
60	Hiden Lake	pollen	Tang, et al. [35]	30	92	-	+
61	Hangzhou	pollen	Huang, et al. [8]	30	120	+	-
62	Mainning	pollen	An, et al. [2]	29	102	+	-
63	Dongting Lake	pollen	Huang, et al. [8]	29	113	+	+
64	Nanchang	pollen	Huang, et al. [8]	29	116	+	+
65	Fanjing Mt.	pollen	Huang, et al. [8]	28	109	-	+
66	Wenzhou	pollen	Huang, et al. [8]	28	121	+	-
67	Eryuan	pollen	An, et al. [2]	26	100	+	-
68	Erhai Lake	TOC	Zhou, et al. [38]	26	110	-	-
69	Kunming	pollen	Huang, et al. [8]	25	103	+	+
70	Dongge Cave	δ13C	Wang, et al. [39]	25	109	+	-
71	Dahu Swamp	TOC	Zhou, et al. [40]	24	115	+	-
72	Fujian	pollen	Huang, et al. [8]	24	118	-	+
73	Taiwan	pollen	Huang, et al. [41]	24	121	+	-
74	Huangsha	pollen	An, et al. [2]	23	110	-	+
75	Fangyu	pollen	An, et al. [2]	23	113	+	+
76	Xishuangbanna	pollen	Huang, et al. [8]	22	110	+	-
77	HuguangyanMaar Lake	dry density	Liu, et al. [42]	21	110	+	+
78	Hainan Island	pollen	Huang, et al. [8]	20	110	+	-
79	South China Sea	salinity	Wang, et al. [43]	20	117	-	-
80	South China Sea	sedimentary rate	Huang, et al.[41]	19	116	-	-

REFERENCES:

[1] CHEN Fa-hu, YU Zi-cheng, YANG Mei-lin, et al. Holocene moisture evolution in arid central Asia and its out-of-phase relationship with Asian monsoon history [J]. Quatern. Sci. Rev., 2008, 27(3-4): 351-364.

[2] AN Z S, WU X H, WANG P X. et al. Paleomonsoons of China over the last 130000 years [J]. Sci. China (Ser. B), 1991, 34(8): 1 016-1 024.

[3] AN C B, FENG Z D, BARTON L. Dry or humid? Mid-Holocene humidity changes in arid and semi-arid China [J]. Quatern. Sci. Rev., 2006, 25: 351-361.

[4] HAN S T, QU Z. Holocene paleoenvironmental reconstruction in the Balikun Lake area [J]. Sci. China (Ser. B), 1992, 11: 1 120-1 201 (in Chinese).

[5] LIU H Y, XU L, CUI H. Holocene history of desertification along the woodland-steppe border in Northern China [J]. Quatern. Res., 2002, 57(2): 259-270.

[6] JIANG Wen-ying, GUO Zheng-tang, SUN Xiang-jun, et al. Reconstruction of climate and vegetation changes of Lake Bayanchagan (Inner Mongolia): Holocene variability of the East Asian monsoon [J]. Quatern. Res., 2006, 65(3): 411-420.

[7] HONG Y T, HONG B, LIN Q H, et al. Inverse phase oscillations between the East Asian and Indian Ocean summer monsoon during the last 12000 years and paleo-El Niño [J]. Earth Planet Sci. Lett., 2005, 231: 337-346.

[8] HUANG Zhen-guo, ZHANG Wei-qiang, et al. Comparative Study of Environmental Evolution during the Holocene in China and Japan [M]. Guangzhou: Guangdong Science and Technology Press, 2002, 1-806 pp.

[9] FENG Q, SU Z Z, JIN H J. Desert evolution and climate changes in the Tarim River Basin during the past 12ka [J]. Sci. China (Ser. D), 1999, 29(suppl.): 87-96.

[10] WANG F Y, SUN X J. Chasuqi peat sequence and the paleoclimatic reconstruction in the Inner Mongolian Plateau [J]. Chin. Sci. Bull., 1997, 42(5): 514-518 (in Chinese).

[11] XIAO Ju-le, WU Jin-tao, SI Bin, et al. Holocene climate changes in the monsoon/arid transition reflected by carbon concentration in Daihai Lake of Inner Mongolia [J]. The Holocene, 2006, 16(4): 551-560.

[12] CHEN C T A, LAU H C, Lou J Y. The dry Holocene Megathermal in Inner-Mongolia [J]. J. Paleogeogr. Palaeoclimatol., Palaeoecol., 2003, 193: 181-200.

[13] CHEN F H, WU W, Holmes J A, et al. A mid-Holocene drought interval as evidenced by lake desiccation in the Alashan Plateau, Inner Mongolia, China [J]. Chin. Sci. Bull., 2003, 48(14): 1 401-1 410.

[14] CHEN Fa-hu, SHI Qi, WANG Jian-min. Environmental

changes documented by sedimentation of Lake Yiema and arid China since the Late Glaciation [J]. J. Paleolimnol., 1999, 22: 159-169.
[15] LIU K B, YAO Z, THOMPSON L G. A pollen record of Holocene climate changes from the Dunde ice cap, Qinghai-Tibetan Plateau [C]// Abstract of the Annual Meeting Association of American Geographers (March 23-26, Los Angeles), 1998.
[16] HERZSCHUH U, ZHANG Cheng-jun, MISCHKE S, et al. A late Quaternary lake record from the Qilian Mountains (NW China): evolution of the primary production and the water depth reconstructed from macrofossil, pollen, biomarker, and isotope data [J]. Global and Planetary Change, 2005, 46: 361-379.
[17] MA Y Z, ZHANG H C, PACHUR H J, et al. Late glacial and Holocene vegetation history and paleoclimate of the Tengger Desert, northwestern China [J]. Chin. Sci. Bull., 2003, 48(14): 1 457-1 462.
[18] CHEN F H, CHENG B, ZHAO Y, et al. Holocene environmental change inferred from a high-resolution pollen record, Lake Zhuyeze, arid China [J]. The Holocene, 2006, 16(5): 675-684.
[19] YIN Chun-min, QIU Wei-li, LI Rong-quan. Holocene paleofloods in the North China Plain [J]. J. Beijing Normal Univ. (Nat. Sci. Edit.), 2001, 37: 280-284.
[20] ZHAO Yan, YU Zi-cheng, CHEN Fa-hu, et al. Holocene vegetation and climate history at Hurleg Lake in the Qaidam Basin northwest China [J]. Rev. Paleobot. Palynol., 2007, 145: 275-288.
[21] LIU X Q, SHEN J, WANG S M. Pollen assemblages and climatic changes in the Qinhai Lake during the past 16ka [J]. Chin. Sci. Bull., 2002, 47(22): 1 931-1 936.
[22] LI X Q, ZHOU W J, AN Z S, et al. The vegetation and monsoon variations at the desert-loess transition belt at Miaiwan in northern China for the last 13ka [J]. The Holocene, 2003, 13: 779-784.
[23] AN C B, TANG L, BARTON L, et al. Climate change and cultural response around 4000 cal yr B. P. in the western part of Chinese Loess Plateau [J]. Quatern. Res., 2005, 63(3): 347-352.
[24] WANG Yong-ji, LI Shan-wei. Paleovegetation and Paleoclimate of Jiaozhou BAY, Qingdao, since 20 000 years [J]. Acta Botan. Sinica, 1983, 25(4): 385-391 (in Chinese).
[25] SHEN Cai-ming, LIU Kam-biu, TANG Lin-yu, et al. Quantitative relationships between modern pollen rain and climate in the Tibetan plateau [J]. Rev. Paleobot. Palynol., 2006, 140(1-2): 61-77.
[26] FONTES J C, GASSE F, GIBERT E. Holocene environmental changes in Lake Bongong basin (Western Tibet). Part1: Chronology and stable isotopes of carbonates of a Holocene lacustrine core [J]. Palaeogr. Palaeoclimatol. Palaeocol., 1996, 120: 25-47.
[27] THOMPSON L G, YAO T, DAVIS M E, et al. Tropical climate instability: the last glacial cycle from a Qinghai- Tibet ice core [J]. Sci., 1997, 276: 1 821-1 825.
[28] PANG Jang-li, HUANG Chun-chang. Study on palaeosol features in Xi'an Area and climatic change during the last 10000 years [J]. Plateau Meteor., 2003, 22: 79-83.
[29] GASSE F, ARNOLD M, JONTES J C, et al. A 13000-year climate record from western Tibet [J]. Nature, 1991, 353: 742-745.
[30] ZHOU W J, LU X F, WU Z K. Peat-recorded climatic variations and the AMS dated chronology in Zoige plateau [J]. Chin. Sci. Bull., 2001, 46: 1 040-1 044.
[31] GU Z Y, LIU J Q, YUAN B Y. Plateau monsoon variations in the Tibetan plateau during the past 12kaBP [J]. Chin. Sci. Bull., 1993, 38: 61-64.
[32] HERZSCHUH U, WINTER K, WÜNNMANN B, et al. A general cooling trend on the central Tibetan Plateau throughout the Holocene record by the Lake Zigetang pollen spectra [J]. Quatern. Internat, 2006, 154-155, 113-121.
[33] MORRILL C, OVERPECK J T, COLE J E, et al. Holocene variations in the Asian monsoon inferred from the geochemistry of lake sediments in central Tibet [J]. Quatern. Res., 2006, 65: 232-243
[34] WU Yan-hong, LÜCKE A, JIN Zhang-dong, et al. Holocene climate development on the central Tibetan Plateau: A sedimentary record Cuoe Lake [J]. Palaeogeogr. Palaeoclimatol. Palaeoecol., 2006, 234: 328-340.
[35] TANG Ling-yn, SHEN Cai-ming, LIU Kam-biu, et al. Changes in South Asian monsoon: New high-resolution paleoclimatic records from Tibet [J]. Chin. Sci. Bull., 2000, 45: 87-91.
[36] SHAO X H, WANG X J, CHENG H, et al. Long-term trend and abrupt events of the Holocene Asian monsoon inferred from a stalagmite $\delta^{18}O$ record from Shennongjiia in central China [J]. Chin. Sci. Bull., 2006, 51: 221-228.
[37] CAI Yong-li, CHEN Zhong-yuan, ZHANG Wei, et al. Climate fluctuation of the western Shanghai District by correspondence analysis since 8.5kaBP [J]. J. Lake Sci., 2001, 13: 118-126.
[38] ZHOU J, WANG S M, YANG G S, et al. The Younger Drays event and the cold events in early-mid Holocene [J]. Adv. Clim. Change Res., 2006, 2: 127-130.
[39] WANG Y J, CHENG H, EDWARDS R L. The Holocene Asian Monsoon: links to solar changes and North Atlantic climate [J]. Sci., 2005, 308: 854-857.
[40] ZHOU Wei-jian, YU Xue-feng, JULL A J T, et al. High-resolution evidence from southern China of an early Holocene optimum and a mid-Holocene dry event during the past 18,000 years [J]. Quatern. Res., 2004, 62: 39-48.
[41] HUANG Chi-Yue, LIEW Ping-Mei, ZHAO Mei-xun, et al. Deep sea and lake records of the Southeast Asian paleomonsoons for the last 25 thousand years [J]. Earth Planet. Sci. Lett., 1997, 146: 59-72.
[42] LIU Jia-qi, LÜ Hou-yuan, NEGENDANK J, et al. Periodicity of Holocene climate variations in the Huguangyan Maar Lake [J]. Chin. Sci. Bull., 2000, 45: 1 712-1 717.
[43] WANG L, SARNTHEIN M, ERLENKEUSER H, et al. East Asian monsoon climate during the Late Pleistocene: high-resolution sediment records from the south China Sea [J]. Mar. Geol., 1999, 156: 245-284.